Machine learning based estimation of axonal permeability: validation on cuprizone treated in-vivo mouse model of axonal demyelination

Marco Palombo[1], Ioana Hill[1], Mathieu Santin[2,3], Francesca Branzoli[2,3], Anne-Charlotte Philippe[2,3], Demian Wassermann[4,5], Marie-Stephane Aigrot[6], Bruno Stankoff[6,7], Hui Zhang[1], Stephan Lehericy[2,3,8], Alexandra Petiet[2,3], Daniel C. Alexander[1], and Ivana Drobnjak[1]

[1]Computer Science Department and Centre for Medical Imaging Computing, University College London, London, United Kingdom, [2]Hôpital de la Pitié Salpêtrière, Sorbonne Universités, UPMC Paris 06 UMR S 1127, Inserm UMR S 1127, CNRS UMR 7225, Institut du Cerveau et de la Moelle épinière, Paris, France, [3]CENIR, Centre de NeuroImagerie de Recherche, CENIR, Paris, France, [4]INRIA, Université Côte d'Azur, Sophia-Antipolis, France, [5]Parietal, CEA, INRIA, Saclay, France, [6]CENIR, Centre de NeuroImagerie de Recherche, Paris, France, [7]AP-HP, Hôpital Saint-Antoine, Paris, France, [8]AP-HP, Hôpital de la Pitié Salpêtrière, Paris, France

Synopsis

Estimating axonal permeability reliably is extremely important, however not yet achieved because mathematical models that express its relationship to the MR signal accurately are intractable. Recently introduced machine learning based computational model showed to outperforms previous approximate mathematical models. Here we apply and validate this novel method experimentally on a highly controlled *in-vivo* mouse model of axonal demyelination, and demonstrate for the first time in practice the power of machine learning as a mechanism to construct complex biophysical models for quantitative MRI.

Introduction

Quantitative MRI relies on biophysical models to relate MR signals to tissue properties, but mathematical models rapidly become intractable beyond very simple descriptions of tissue, and parameters such as permeability remain elusive. A recent study[1] demonstrated that using machine learning we can construct a computational model that outperforms approximate mathematical models in estimating permeability via the residence time τ_i of water inside axons. τ_i is a potentially important biomarker for white matter pathologies, as myelin damage is hypothesized to affect axonal permeability, and thus τ_i.

Here we for the first time apply and validate this novel idea on a highly controlled *in-vivo* mouse model of axonal demyelination. We use Monte Carlo simulations and random forest (RF) regression[1] to build a mapping between diffusion-weighted MR signals and ground-truth microstructure parameters. We then estimate differences in τ_i between *in-vivo* healthy and cuprizone-treated (CPZ) mice brain, a well-known model of white matter (WM) demyelination.

Methods

In-vivo data. We used a diffusion-weighted Pulsed-Gradients-Spin-Echo (DW-PGSE) protocol (**Tab.1**). We scanned sixteen C57BL6J mice on BrukerBioSpec 11.7T: eight CPZ mice at 6 weeks post intoxication (0.2% cuprizone) and eight healthy age-matched wild-type (WT) mice of the same background (data available on https://zenodo.org/record/996889#.WgH5E9vMx24). Images are corrected for eddy-currents using FSL-eddy. DTI and NODDI[2] maps are computed for comparison.

Simulation data. We used MC simulations in CAMINO[3]. To mimic the *in-vivo* mouse brain, WM was modelled as a collection of non-abutting parallel cylinders with gamma-distributed radii with parameters randomly selected for 11000 substrates in the ranges: mean and standard deviation of axonal radius $\mu_R \in [0.1,1.0]\mu m$ and $\sigma_R \in [\min(0.1,\mu_R/5),\mu_R/2]\mu m$, intra-axonal volume fraction $f_i \in [0.40,0.75]$, $\tau_i \in [0.02,1.00]s$, intrinsic diffusivity $d \in [0.8,2.2]\mu m^2/ms$. Signal-to-noise ratio 30.

Data quality test. We assessed the sensitivity of our imaging protocol to τ_i using synthetic data as in[4], and the quality of the synthetic data by direct comparison with the *in-vivo* data.

Machine Learning. We adapted the well-known RF regressor in the scikit-learn toolkit[5] to learn the mapping between the microstructure parameters defining our simulation substrates and the normalized DW-MRI signal (**Fig.1**). The RF had decision trees/maximum depth=100/20. We trained the RF on simulated data using 11000 feature vectors (synthetic diffusion-weighted signals) through a greedy splitting process that constructs a linear mapping from the features to the corresponding ground truth parameters. The trained RF estimates f_i, τ_i and d, which we tested on simulated data using 1500 previously unseen feature vectors and then applied on *in-vivo* data. We manually segmented the corpus callosum (CC) and Fornix and compared WT and CPZ mice estimates using 2-tailed t-test with equal variance.

Results

Data quality test. **Fig.2A** shows that our imaging protocol has good sensitivity to τ_i, with sufficient change in DW-MRI signal to provide reliable τ_i estimates for $\tau_i \leq 500$ ms. **Fig.2B** shows an excellent match between the simulated and *in-vivo* diffusion-weighted signals, demonstrating that our training data set is a good representation of the *in-vivo* data.

Simulation data estimates. Testing shows strong correlations between RF estimates and the ground truth parameters (R^2=0.86/0.94/0.88 for f_i/τ_i/d respectively). A comprehensive sensitivity/accuracy analysis of the proposed method is the subject of another abstract that we submitted to this symposium.

Machine Learning. **Fig.3** shows parametric maps from the *in-vivo* data (WT versus CPZ) of conventional DTI, NODDI orientation-dispersion index (ODI) and using RF approach. RF estimates in CPZ mice show a statistical significant reduction in f_i, and τ_i compared to WT (**Fig.4**). DTI shows reduction in FA and increase in RD, in agreement with[6]. ODI is not statistical different between the two groups (**Fig.4**). An electron microscopy image of CC is also reported to show the underpinning microstructural changes in the tissue: demyelination and partial axonal loss.

Discussion and Conclusion

Our analysis of DW-MRI from a well-known mouse model of WM demyelination **(Fig.3,4)** shows that machine learning approach allows an accurate and robust estimation of the expected changes in tissue-microstructure. While DTI gave only indirect information, our model found: 1) a decrease in f_i as direct measure of partial axonal loss; 2) a decrease in τ_i as direct measure of axonal membrane permeability increase due to demyelination. Furthermore, our estimates show no bias due to fiber orientation dispersion, as shown by the negligible changes in ODI. Finally, our results match the expected tissue-microstructure changes (electron microscopy in **Fig.3**).

Standard methods for estimating permeability so far have been using the Karger model[7], however in[1] has been shown that machine learning approach works much better. Here we provide a clear validation of the machine learning approach introduced in[1] affirming a wider potential of the approach as a mechanism to construct complex biophysical models for quantitative MRI.

Acknowledgements

This work was supported by EPSRC (EP/G007748, EP/I027084/01, EP/L022680/1, EP/M020533/1, N018702), EPSRC-funded UCL Centre for Doctoral Training in Medical Imaging (EP/L016478/1), Spinal Research, UK MS Society and NIHR Biomedical Research Centre at University College London Hospitals. The research leading to these results received funding from the programs 'Institut des neurosciences translationnelle' ANR-10-IAIHU-06 and 'Infrastructure d'avenir en Biologie Santé' ANR-11-INBS-0006.

References

[1] Nedjati-Gilani, G.L., Schneider, T., Hall, M.G., Cawley, N., Hill, I., Ciccarelli, O., Drobnjak, I., Wheeler-Kingshott, C.A.M.G., Alexander, D.C. : Machine learning based compartment models with permeability for white matter microstructure imaging, NeuroImage, http://dx.doi.org/10.1016/j.neuroimage.2017.02.013 (2017).

[2] Zhang G, et al. NODDI: practical in vivo neurite orientation dispersion and density imaging of the human brain. Neuroimage 2012; 61 (4): 1000-1016.

[3] Cook, P. A., Bai, Y., Nedjati-Gilani, S., Seunarine, K.K., Hall, M.G., Parker, G.J., Alexander, D.C. : Camino: Open-Source Diffusion-MRI Reconstruction and Processing, 14th Scientific Meeting of the International Society for Magnetic Resonance in Medicine, Seattle, WA, USA, p. 2759, May 2006.

[4] Drobnjak, I., Zhang, H., Ianuş, A., Kaden, E., & Alexander, D. C.: PGSE, OGSE, and sensitivity to axon diameter in diffusion MRI: Insight from a simulation study. Magnetic resonance in medicine, 75 (2), 688-700 (2015)

[5] Pedregosa, F., Varoquaux, G., Gramfort, A., Michel, V., Thirion, B., Grisel, O., Blondel, M., Prettenhofer, P., Weiss, R., Dubourg, V., Vanderplas, J., Passos, A., Cournapeau, D., Brucher, M., Perrot, M., Duchesnay, E.: Scikit-learn: Machine Learning in Python. JMLR 12, 2825-30 (2011).

[6] Zhang, J., Jones, M. V., McMahon, M. T., Mori, S., Calabresi, P. A. : In vivo and ex vivo diffusion tensor imaging of cuprizone-induced demyelination in the mouse corpus callosum. Magnetic resonance in medicine, 67(3), 750-759 (2012).

[7] Karger, J., Pfeifer, H., Wilfried, H.: Principles and application of self-diffusion measurements by nuclear magnetic resonance. Adv Mag Res 12(1), 1-89 (1988)

Figures

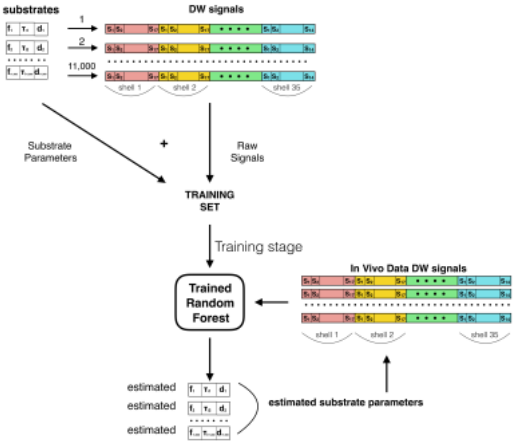

Fig.1 A schematic overview of how testing, training and estimation is done with random forest regression.

DW-MRI PGSE-EPI sequence parameters	
TE	33.6 ms
TR	2000 ms
Diffusion gradient duration	5 ms
Diffusion gradient separation	10.8, 13.1, 15.4, 17.7, 20.0 ms
Diffusion gradient strength	50, 100, 150, 200, 300, 400, 500 mT/m
# Diffusion gradient direction	16, 16, 16, 16, 8, 11, 13
FOV	16x16 mm
Matrix size	160x160
Number of Slices	5
Slice thickness	0.5 mm

Tab.1 Summary of the PGSE EPI sequence parameters used to simulate and acquire data.

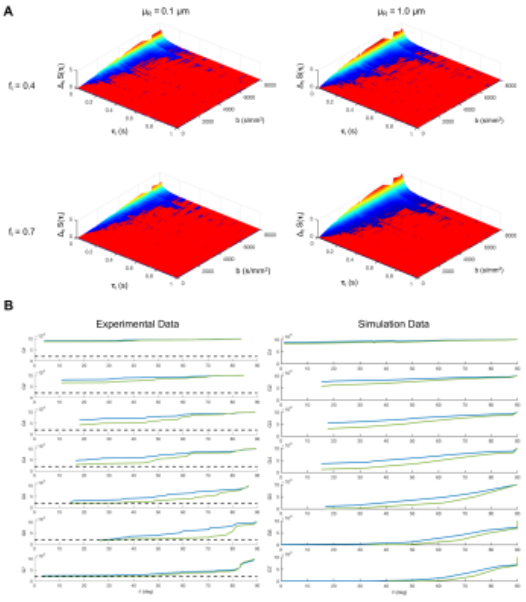

Fig.2 A) DW-MR signal sensitivity to changes in τ_i, for different tissue substrates simulated (f_i = 0.4,0.7; μ_R=0.1,1.0 μm). Sensitivity is defined as $\Delta_h S(\tau_i) = |S(\tau_i)-S(\tau_i+h)| / h$, where h was set equal to 0.05 s. Red planes denote the noise level. B) Comparison between experimental and simulated signal intensity as a function of the angle between the diffusion gradients and the cylindrical fibres axis θ (in degrees), for different diffusion gradient strength, $G_{1\text{-}7}$ = 50-500 mT/m, and diffusion gradient separation Δ=10.8 ms (blue lines) and 20.0 ms (green lines). Dashed black line in experimental data represent the noise level.

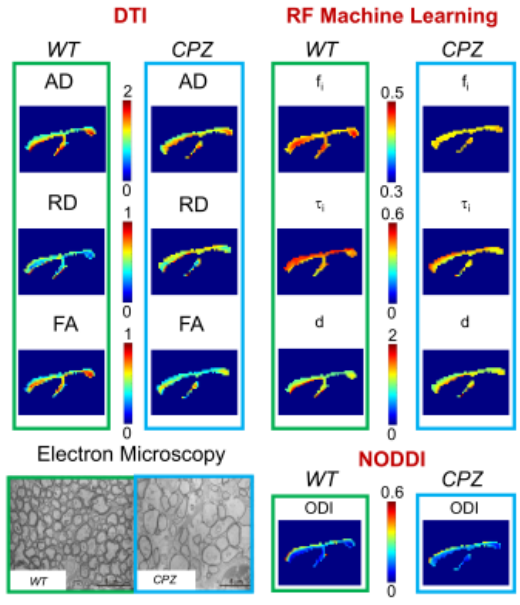

Fig.3 Parametric maps obtained from conventional DTI at b=1500 s/mm^2 (axial and radial diffusivity, AD and RD, and fractional anisotropy FA), RF approach (f_i, τ_i, d) and NODDI ODI. Diffusivities are in μm^2/ms and τ_i in seconds. The mask of the CC (and Fornix) is obtained by applying the

following constraints: $C_l=(\lambda_1-\lambda_2)/\lambda_1>0.5$, $C_p=(\lambda_2-\lambda_3)/\lambda_1<0.3$, third component of the main DTI eigenvector, $|e_1^{(3)}|>0.8$. Some partial volume effects are visible at the border of the masked regions. For this reason, only the central portions of the masked CC and Fornix were considered for the statistical analysis in **Fig.4**.

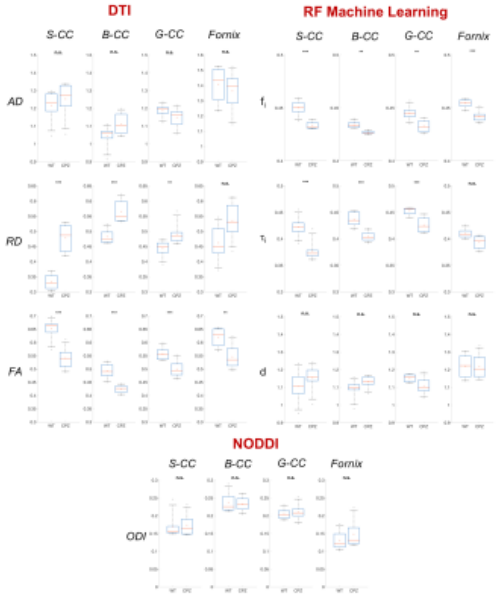

Fig.4 Box-and-whisker plots of region-specific comparison between WT (N=8) and CPZ (N=8). DTI metrics (AD, RD, FA), RF metrics (f_i, τ_i, d) and NODDI ODI were evaluated within the splenium (S-CC), body (B-CC) and genu (G-CC) of the Corpus Callosum (CC) and Fornix. Statistical significance was assessed by using 2-tailed t-test with equal variance and significance level *=0.01,**=0.005,***=0.001. N.s. stands for non-significant.